



# The Cheng–Minkowycz problem for natural convective boundary-layer flow in a porous medium saturated by a nanofluid

D.A. Nield<sup>a</sup>, A.V. Kuznetsov<sup>b,\*</sup>

<sup>a</sup> Department of Engineering Science, University of Auckland, Private Bag 92019, Auckland 1142, New Zealand

<sup>b</sup> Department of Mechanical and Aerospace Engineering, North Carolina State University, Campus Box 7910, Raleigh, NC 27695-7910, USA

## ARTICLE INFO

### Article history:

Received 14 April 2009

Received in revised form 31 July 2009

Accepted 31 July 2009

Available online 11 September 2009

### Keywords:

Cheng–Minkowycz problem

Natural convection

Nanofluid

Porous medium

Similarity solution

## ABSTRACT

The Cheng–Minkowycz problem of natural convection past a vertical plate, in a porous medium saturated by a nanofluid, is studied analytically. The model used for the nanofluid incorporates the effects of Brownian motion and thermophoresis. For the porous medium the Darcy model is employed. A similarity solution is presented. This solution depends on a Lewis number  $Le$ , a buoyancy-ratio number  $Nr$ , a Brownian motion number  $Nb$ , and a thermophoresis number  $Nt$ . The dependency of the Nusselt number on these four parameters is investigated.

© 2009 Elsevier Ltd. All rights reserved.

## 1. Introduction

The term “nanofluid” refers to a liquid containing a dispersion of submicronic solid particles (nanoparticles). The term was coined by Choi [1]. The characteristic feature of nanofluids is thermal conductivity enhancement, a phenomenon observed by Masuda et al. [2]. This phenomenon suggests the possibility of using nanofluids in advanced nuclear systems (Buongiorno and Hu [3]).

A comprehensive survey of convective transport in nanofluids was made by Buongiorno [4], who says that a satisfactory explanation for the abnormal increase of the thermal conductivity and viscosity is yet to be found. He focused on the further heat transfer enhancement observed in convective situations. Buongiorno notes that several authors have suggested that convective heat transfer enhancement could be due to the dispersion of the suspended nanoparticles but he argues that this effect is too small to explain the observed enhancement. Buongiorno also concludes that turbulence is not affected by the presence of the nanoparticles so this cannot explain the observed enhancement. Particle rotation has also been proposed as a cause of heat transfer enhancement, but Buongiorno calculates that this effect is too small to explain the effect. With dispersion, turbulence and particle rotation ruled out as significant agencies for heat transfer enhancement, Buongiorno

proposed a new model based on the mechanics of the nanoparticle/base-fluid relative velocity.

Buongiorno [4] noted that the nanoparticle absolute velocity can be viewed as the sum of the base fluid velocity and a relative velocity (that he calls the slip velocity). He considered in turn seven slip mechanisms: inertia, Brownian diffusion, thermophoresis, diffusiophoresis, Magnus effect, fluid drainage, and gravity settling. After examining each of these in turn, he concluded that in the absence of turbulent effects it is the Brownian diffusion and the thermophoresis that will be important. Buongiorno proceeded to write down conservation equations based on these two effects.

The problem of natural convection in a porous medium past a vertical plate is a classical problem first studied by Cheng and Minkowycz [5]. The problem is presented as a paradigmatic configuration and solution in the book by Bejan [6]. The extension to the case of heat and mass transfer was made by Bejan and Khair [7]. Further work on this topic is surveyed in Sections 5.1 and 9.2.1 in Nield and Bejan [8]. A review of the heat transfer characteristics of nanofluids has been made by Wang and Mujumdar [9].

In the present paper the model of [4] is applied to the problem in [5].

## 2. Analysis

It is assumed that nanoparticles are suspended in the nanofluid using either surfactant or surface charge technology. This prevents particles from agglomeration and deposition on the porous matrix.

\* Corresponding author.

E-mail addresses: [d.nield@auckland.ac.nz](mailto:d.nield@auckland.ac.nz) (D.A. Nield), [avkuznet@eos.ncsu.edu](mailto:avkuznet@eos.ncsu.edu) (A.V. Kuznetsov).

## Nomenclature

$D_B$	Brownian diffusion coefficient	$(x, y)$	Cartesian coordinates ( $x$ -axis is aligned vertically upwards, plate is at $y = 0$ )
$D_T$	thermophoretic diffusion coefficient	<b>Greek symbols</b>	
$f$	rescaled nanoparticle volume fraction, defined by Eq. (20)	$\alpha_m$	thermal diffusivity of the porous medium, $\frac{k_m}{(\rho c)_f}$
$\mathbf{g}$	gravitational acceleration vector	$\beta$	volumetric expansion coefficient of the fluid
$k_m$	effective thermal conductivity of the porous medium	$\varepsilon$	porosity
$K$	permeability of the porous medium	$\eta$	similarity variable, defined by Eq. (19)
$Le$	Lewis number, defined by Eq. (27)	$\theta$	dimensionless temperature, defined by Eq. (20)
$Nr$	buoyancy ratio, defined by Eq. (24)	$\mu$	viscosity of the fluid
$Nb$	Brownian motion parameter, defined by Eq. (25)	$\rho_f$	fluid density
$Nt$	thermophoresis parameter, defined by Eq. (26)	$\rho_p$	nanoparticle mass density
$Nu$	Nusselt number, defined by Eq. (32)	$(\rho c)_f$	heat capacity of the fluid
$Nur$	reduced Nusselt number, $Nu/Ra_x^{1/2}$	$(\rho c)_m$	effective heat capacity of the porous medium
$p$	pressure	$(\rho c)_p$	effective heat capacity of the nanoparticle material
$q''$	wall heat flux	$\tau$	parameter defined by Eq. (13), $\frac{\varepsilon(\rho c)_p}{(\rho c)_f}$
$Ra_x$	local Rayleigh number, defined by Eq. (18)	$\phi$	nanoparticle volume fraction
$s$	dimensionless stream function, defined by Eq. (20)	$\phi_w$	nanoparticle volume fraction at the vertical plate
$T$	temperature	$\phi_\infty$	ambient nanoparticle volume fraction attained as $y$ tends to infinity
$T_w$	temperature at the vertical plate	$\psi$	stream function, defined by Eq. (14)
$T_\infty$	ambient temperature attained as $y$ tends to infinity		
$\mathbf{v}$	Darcy velocity, $(u, v)$		

We consider a two-dimensional problem. We select a coordinate frame in which the  $x$ -axis is aligned vertically upwards. We consider a vertical plate at  $y = 0$ . At this boundary the temperature  $T$  and the nanoparticle fraction  $\phi$  take constant values  $T_w$  and  $\phi_w$ , respectively. The ambient values, attained as  $y$  tends to infinity, of  $T$  and  $\phi$  are denoted by  $T_\infty$  and  $\phi_\infty$ , respectively.

The Oberbeck-Boussinesq approximation is employed. Homogeneity and local thermal equilibrium in the porous medium is assumed. We consider a porous medium whose porosity is denoted by  $\varepsilon$  and permeability by  $K$ . The Darcy velocity is denoted by  $\mathbf{v}$ . The following four field equations embody the conservation of total mass, momentum, thermal energy, and nanoparticles, respectively. The field variables are the Darcy velocity  $\mathbf{v}$ , the temperature  $T$  and the nanoparticle volume fraction  $\phi$ .

$$\nabla \cdot \mathbf{v} = 0, \quad (1)$$

$$\frac{\rho_f}{\varepsilon} \frac{\partial \mathbf{v}}{\partial t} = -\nabla p - \frac{\mu}{K} \mathbf{v} + [\phi \rho_p + (1 - \phi) \{ \rho_f (1 - \beta(T - T_\infty)) \}] \mathbf{g}, \quad (2)$$

$$(\rho c)_m \frac{\partial T}{\partial t} + (\rho c)_f \mathbf{v} \cdot \nabla T = k_m \nabla^2 T + \varepsilon (\rho c)_p [D_B \nabla \phi \cdot \nabla T + (D_T/T_\infty) \nabla T \cdot \nabla T], \quad (3)$$

$$\frac{\partial \phi}{\partial t} + \frac{1}{\varepsilon} \mathbf{v} \cdot \nabla \phi = D_B \nabla^2 \phi + (D_T/T_\infty) \nabla^2 T. \quad (4)$$

We write  $\mathbf{v} = (u, v)$ .

Here  $\rho_f$ ,  $\mu$  and  $\beta$  are the density, viscosity, and volumetric volume expansion coefficient of the fluid while  $\rho_p$  is the density of the particles. The gravitational acceleration is denoted by  $\mathbf{g}$ . We have introduced the effective heat capacity  $(\rho c)_m$ , and the effective thermal conductivity  $k_m$  of the porous medium. The coefficients that appear in Eqs. (3) and (4) are the Brownian diffusion coefficient  $D_B$  and the thermophoretic diffusion coefficient  $D_T$ . Details of the derivation of Eqs. (3) and (4) are given in the papers by Buongiorno [4], Tzou [10,11] and Nield and Kuznetsov [12,13]. The flow is assumed to be slow so that an advective term and a Forchheimer quadratic drag term do not appear in the momentum equation.

The boundary conditions are taken to be

$$v = 0, \quad T = T_w, \phi = \phi_w \text{ at } y = 0, \quad (5)$$

$$u = v = 0, \quad T \rightarrow T_\infty, \phi \rightarrow \phi_\infty \text{ as } y \rightarrow \infty. \quad (6)$$

We consider a steady state flow.

In keeping with the Oberbeck-Boussinesq approximation and an assumption that the nanoparticle concentration is dilute, and with a suitable choice for the reference pressure, we can linearize the momentum equation and write Eq. (2) as

$$0 = -\nabla p - \frac{\mu}{K} \mathbf{v} + [(\rho_p - \rho_{f\infty})(\phi - \phi_\infty) + (1 - \phi_\infty)\rho_{f\infty}\beta(T - T_\infty)] \mathbf{g}. \quad (7)$$

We now make the standard boundary-layer approximation, based on a scale analysis, and write the governing equations

$$\frac{\partial u}{\partial x} + \frac{\partial v}{\partial y} = 0, \quad (8)$$

$$\frac{\partial p}{\partial x} = -\frac{\mu}{K} u + [(1 - \phi_\infty)\rho_{f\infty}\beta g(T - T_\infty) - (\rho_p - \rho_{f\infty})g(\phi - \phi_\infty)] \quad (9)$$

$$\frac{\partial p}{\partial y} = 0, \quad (10)$$

$$u \frac{\partial T}{\partial x} + v \frac{\partial T}{\partial y} = \alpha_m \nabla^2 T + \tau \left[ D_B \frac{\partial \phi}{\partial y} \frac{\partial T}{\partial y} + \left( \frac{D_T}{T_\infty} \right) \left( \frac{\partial T}{\partial y} \right)^2 \right], \quad (11)$$

$$\frac{1}{\varepsilon} \left( u \frac{\partial \phi}{\partial x} + v \frac{\partial \phi}{\partial y} \right) = D_B \frac{\partial^2 \phi}{\partial y^2} + \left( \frac{D_T}{T_\infty} \right) \frac{\partial^2 T}{\partial y^2}. \quad (12)$$

where

$$\alpha_m = \frac{k_m}{(\rho c)_f}, \quad \tau = \frac{\varepsilon(\rho c)_p}{(\rho c)_f}. \quad (13)$$

One can eliminate  $p$  from Eqs. (9) and (10) by cross-differentiation. At the same time one can introduce a stream function  $\psi$  defined by

$$u = \frac{\partial \psi}{\partial y}, \quad v = -\frac{\partial \psi}{\partial x}, \quad (14)$$

so that Eq. (8) is satisfied identically. We are then left with the following three equations.

$$\frac{\partial^2 \psi}{\partial y^2} = \frac{(1 - \phi_\infty)\rho_{f\infty}\beta g K}{\mu} \frac{\partial T}{\partial y} - \frac{(\rho_p - \rho_{f\infty})g K}{\mu} \frac{\partial \phi}{\partial y} \quad (15)$$

$$\frac{\partial \psi}{\partial y} \frac{\partial T}{\partial x} - \frac{\partial \psi}{\partial x} \frac{\partial T}{\partial y} = \alpha_m \nabla^2 T + \tau \left[ D_B \frac{\partial \phi}{\partial y} \frac{\partial T}{\partial y} + \left( \frac{D_T}{T_\infty} \right) \left( \frac{\partial T}{\partial y} \right)^2 \right], \quad (16)$$

$$\frac{1}{\varepsilon} \left( \frac{\partial \psi}{\partial y} \frac{\partial \phi}{\partial x} - \frac{\partial \psi}{\partial x} \frac{\partial \phi}{\partial y} \right) = D_B \frac{\partial^2 \phi}{\partial y^2} + \left( \frac{D_T}{T_\infty} \right) \frac{\partial^2 T}{\partial y^2}. \quad (17)$$

We now introduce the local Rayleigh number  $Ra_x$  defined by

$$Ra_x = \frac{(1 - \phi_\infty)\rho_{f\infty}\beta g K x}{\mu \alpha_m}, \tag{18}$$

and the similarity variable

$$\eta = \frac{y}{x} Ra_x^{1/2}. \tag{19}$$

This choice is made on the basis of scale analysis (see Section 9.2.1 of Nield and Bejan [8]). Since most nanofluids examined to date have large values for the Lewis number, we are interested mainly in the case  $Le > 1$ . Also we are interested in the case where it is heat transfer (rather than mass transfer) that is driving the flow. In the present context this means that we are assuming that the buoyancy-ratio parameter  $Nr$  defined by Eq. (24) below is small compared with unity and that the Lewis number  $Le$  defined by Eq. (27) is larger than unity. The reader is referred to Figure 9.5 and Table 9.1 in [8], which are based on Figure 2 and Table 1 in [7].

We also introduce the dimensionless variables  $s$ ,  $\theta$ , and  $f$  defined by

$$s(\eta) = \frac{\psi}{\alpha_m Ra_x^{1/2}}, \quad \theta(\eta) = \frac{T - T_\infty}{T_w - T_\infty}, \quad f(\eta) = \frac{\phi - \phi_\infty}{\phi_w - \phi_\infty}. \tag{20}$$

Then, on substitution in Eqs. (15)–(17), we obtain the ordinary differential equations

$$s'' - \theta' + Nr f' = 0, \tag{21}$$

$$\theta'' + \frac{1}{2} s \theta' + Nb f' \theta' + Nt \theta^2 = 0, \tag{22}$$

$$f'' + \frac{1}{2} Le s f' + \frac{Nt}{Nb} \theta'' = 0, \tag{23}$$

where the four parameters are defined by

$$Nr = \frac{(\rho_p - \rho_{f\infty})(\phi_w - \phi_\infty)}{\rho_{f\infty}\beta(T_w - T_\infty)(1 - \phi_\infty)}, \tag{24}$$

$$Nb = \frac{\varepsilon(\rho c)_p D_B (\phi_w - \phi_\infty)}{(\rho c)_f \alpha_m}, \tag{25}$$

$$Nt = \frac{\varepsilon(\rho c)_p D_T (T_w - T_\infty)}{(\rho c)_f \alpha_m T_\infty}, \tag{26}$$

$$Le = \frac{\alpha_m}{\varepsilon D_B}. \tag{27}$$

Here  $Nr$ ,  $Nb$ ,  $Nt$ ,  $Le$  denote a buoyancy ratio, a Brownian motion parameter, a thermophoresis parameter, and a Lewis number, respectively.

Equations (21)–(23) are solved subject to the following boundary conditions:

$$\text{At } \eta = 0 : s = 0, \quad \theta = 1, \quad f = 1. \tag{28}$$

$$\text{As } \eta \rightarrow \infty : s' = 0, \quad \theta = 0, \quad f = 0. \tag{29}$$

Integrating Eq. (21) once and using boundary conditions (29) results in

$$s' - \theta + Nr f = 0, \tag{30}$$

Equations (30), (22), and (23) are solved subject to boundary conditions at  $\eta = 0$  given by Eq. (28) and the following boundary conditions at  $\eta \rightarrow \infty$ :

$$\text{At } \eta \rightarrow \infty : \theta = 0, \quad f = 0. \tag{31}$$

When  $Nr$ ,  $Nb$  and  $Nt$  are all zero, Eqs. (21) and (22) involve just two dependent variables, namely  $s$  and  $\theta$ , and the boundary-value problem for these two variables reduces to the classical problem solved by Cheng and Minkowycz [5]. (The boundary-value problem for  $f$  then becomes ill-posed and is of no physical significance.)

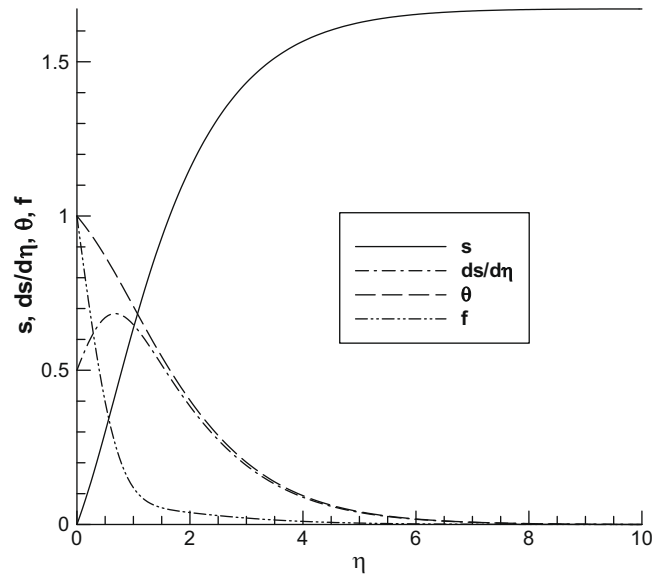


Fig. 1. Plots of dimensionless similarity functions  $s(\eta)$ ,  $s'(\eta)\theta(\eta)$ ,  $f(\eta)$  for the case  $Le = 10$ ,  $Nr = 0.5$ ,  $Nb = 0.5$ ,  $Nt = 0.5$ .

A quantity of practical interest is the Nusselt number  $Nu$  defined by

$$Nu = \frac{q'' x}{k_m (T_w - T_\infty)}, \tag{32}$$

where  $q''$  is the wall heat flux and  $k_m$  is the effective thermal conductivity of the porous medium. In the present context  $Nu/Ra_x^{1/2}$  is represented by  $-\theta'(0)$ . (Likewise the dimensionless mass flux is represented by a Sherwood number  $Sh$  which is proportional to  $-f'(0)$ , but this of lesser interest here.)

### 3. Results and discussion

Plots of the similarity variables for a typical case, chosen as that for  $Le = 10$ ,  $Nr = 0.5$ ,  $Nb = 0.5$ ,  $Nt = 0.5$ , are shown in Fig. 1. The boundary-layer profiles for the temperature function  $\theta(\eta)$  and the stream function  $s(\eta)$  have essentially the same form as in the case of a regular fluid. The thickness of the boundary-layer for the mass fraction function  $f(\eta)$  is smaller than the thermal boundary-layer thickness when  $Le > 1$ . It is well known that, in the case of a regular fluid, the profile for  $ds/d\eta$  (something that represents the longitudinal component of the velocity,  $u$ ) is identical with that for the temperature  $\theta$ . We now see that in the case of a nanofluid the two profiles diverge within a layer whose thickness is comparable with that of the mass fraction.

Table 1

Linear regression coefficients and error bound for the reduced Nusselt number. Here  $C_r$ ,  $C_b$ ,  $C_t$  are the coefficients in the linear regression estimate  $Nu_{est}/Ra_x^{1/2} = 0.444 + C_r Nr + C_b Nb + C_t Nt$ , and  $\hat{\varepsilon}$  is the maximum relative error defined by  $\hat{\varepsilon} = |(Nu_{est} - Nu)/Nu|$ , applicable for  $Nr$ ,  $Nb$ ,  $Nt$  each in  $[0, 0.5]$ .

Le	$C_r$	$C_b$	$C_t$	$\hat{\varepsilon}$
1	-0.309	-0.060	-0.166	0.154
2	-0.230	-0.129	-0.162	0.147
5	-0.148	-0.209	-0.152	0.126
10	-0.111	-0.245	-0.150	0.119
20	-0.086	-0.268	-0.149	0.114
50	-0.064	-0.288	-0.149	0.110
100	-0.053	-0.298	-0.148	0.108
200	-0.045	-0.304	-0.148	0.107
500	-0.039	-0.310	-0.148	0.106
1000	-0.036	-0.313	-0.148	0.107

**Table 2**

Quadratic regression coefficients and error bound for the reduced Nusselt number. Here  $C_{r1}$ ,  $C_{r2}$ ,  $C_{b1}$ ,  $C_{b2}$ ,  $C_{t1}$ ,  $C_{t2}$ ,  $C_{bt}$ ,  $C_{tr}$ , and  $C_{rb}$  are the coefficients in the quadratic regression estimate  $Nu_{est}/Ra_x^{1/2} = 0.444 + C_{r1}Nr + C_{b1}Nb + C_{t1}Nt + C_{r2}Nr^2 + C_{b2}Nb^2 + C_{t2}Nt^2 + C_{bt}NbNt + C_{tr}NtNr + C_{rb}NrNb$ , and  $\hat{\epsilon}$  is the maximum relative error defined by  $\hat{\epsilon} = |(Nu_{est} - Nu)/Nu|$ , applicable for  $Nr$ ,  $Nb$ ,  $Nt$  each in  $[0, 0.5]$ .

Le	$C_{r1}$	$C_{b1}$	$C_{t1}$	$C_{r2}$	$C_{b2}$	$C_{t2}$	$C_{bt}$	$C_{tr}$	$C_{rb}$	$\hat{\epsilon}$
1	-0.353	-0.020	-0.223	-0.040	-0.381	0.067	0.284	-0.122	0.451	0.066
2	-0.249	-0.130	-0.206	-0.066	-0.279	0.040	0.268	-0.102	0.397	0.100
5	-0.160	-0.251	-0.192	-0.028	-0.064	0.042	0.162	-0.014	0.206	0.035
10	-0.115	-0.306	-0.189	-0.016	0.017	0.042	0.135	0.007	0.134	0.014
20	-0.083	-0.344	-0.187	-0.009	0.065	0.041	0.124	0.0135	0.091	0.007
50	-0.055	-0.375	-0.186	-0.004	0.103	0.041	0.121	0.014	0.056	0.007
100	-0.041	-0.390	-0.186	-0.001	0.119	0.041	0.121	0.013	0.040	0.006
200	-0.031	-0.400	-0.185	0.001	0.130	0.041	0.121	0.012	0.029	0.006
500	-0.022	-0.409	-0.185	0.003	0.139	0.041	0.122	0.010	0.020	0.006
1000	-0.018	-0.413	-0.185	0.004	0.143	0.041	0.123	0.009	0.016	0.006

For the case  $Le = 10$ , the value of  $Nu/Ra_x^{1/2}$  (something that we will refer to as the reduced Nusselt number and denote by  $Nur$ ) was calculated for 125 sets of values of  $Nr$ ,  $Nb$ ,  $Nt$  in the range  $[0.1, 0.2, 0.3, 0.4, 0.5]$  and a linear regression was performed on the results. This yielded the correlation

$$Nur_{est} = 0.444 - 0.111Nr - 0.245Nb - 0.150Nt, \quad (33)$$

valid for  $Nr$ ,  $Nb$ ,  $Nt$  each taking values in the range  $[0, 0.5]$ , with a maximum error of about 12%. Clearly an increase in any of the buoyancy-ratio number  $Nr$ , the Brownian motion parameter  $Nb$ , or the thermophoresis parameter  $Nt$  leads to a decrease in the value of the reduced Nusselt number (corresponding to an increase in the thermal boundary-layer thickness). The maximum error occurs at the extreme end of the range considered, namely when  $(Nr, Nb, Nt) = (0.5, 0.5, 0.5)$ , and the correlation formula overestimates the reduction from the standard fluid value 0.444.

This exercise was repeated for other values of  $Le$ , with the results shown in Table 1.

These results show that the coefficient of  $Nt$  varies little as  $Le$  varies. This result is to be expected since, from the form of Eq. (23), one can anticipate that when  $Le$  is large the variable  $f'$  will decay rapidly as  $\eta$  increases, and then since the term in  $Nt$  in Eq. (22) does not involve  $f$  one can anticipate that the contribution from  $Nt$  will not depend markedly on the value of  $Le$ . On the other hand, the coefficient of  $Nr$  decreases markedly as  $Le$  increase while the coefficient of  $Nt$  changes in the other direction. Finally from Table 1 we observe that the accuracy of the linear regression estimate increases as  $Le$  increases.

We believe that for most practical purposes the simple linear regression formula in Eq. (33) should be adequate. If one wants a more accurate formula then one can perform a quadratic regression. For the case  $Le = 10$ , for example, we obtained instead of Eq. (33) the formula

$$Nur_{est} = 0.444 - 0.115Nr - 0.306Nb - 0.189Nt - 0.016Nr^2 + 0.017Nb^2 + 0.042Nt^2 + 0.135NbNt + 0.007NtNr + 0.134NrNb, \quad (34)$$

which gives a maximum error of just 1.4% over the same range. The relatively large interactions between  $Nr$  and  $Nb$  (displayed by the coefficient of the last term in Eq. (34)), and between  $Nr$  and  $Nt$  (displayed by the coefficient of the third to last term in Eq. (34)) are of interest. Values of the coefficients for some other cases are presented in Table 2.

## 4. Conclusions

We have examined the influence of nanoparticles on natural convection boundary-layer flow in a porous medium past a vertical plate, using a model in which Brownian motion and thermophoresis are accounted for. In this pioneering study we have employed the Darcy model for the momentum equation and we have assumed the simplest possible boundary conditions, namely those in which both the temperature and the nanoparticle fraction are constant along the wall. This permits a simple similarity solution which depends on four dimensionless parameters, namely a Lewis number  $Le$ , a buoyancy-ratio parameter  $Nr$ , a Brownian motion parameter  $Nb$ , and a thermophoresis parameter  $Nt$ . We have explored the way in which the wall heat flux, represented by a Nusselt number  $Nu$ , depends on these four parameters. Since we are dealing with the case of convection driven mainly by heat transfer we expect that the boundary condition on the nanoparticle fraction is of lesser importance.

## References

- [1] S. Choi, Enhancing thermal conductivity of fluids with nanoparticle, in: D.A. Siginer, H.P. Wang, (Eds.), Developments and Applications of Non-Newtonian Flows, ASME FED - vol. 231, MD - vol. 66, 1995, pp. 99–105.
- [2] H. Masuda, A. Ebata, K. Teramae, N. Hishinuma, Alteration of thermal conductivity and viscosity of liquid by dispersing ultra-fine particles, *Netsu Bussei* 7 (1993) 227–233.
- [3] J. Buongiorno, W. Hu, Nanofluid coolants for advanced nuclear power plants, in: Proceedings of ICAPP '05, Paper no. 5705, Seoul, May 15–19, 2005.
- [4] J. Buongiorno, Convective transport in nanofluids, *ASME J. Heat Transfer* 128 (2006) 240–250.
- [5] P. Cheng, W.J. Minkowycz, Free convection about a vertical flat plate embedded in a porous medium with application to heat transfer from a dike, *J. Geophys. Res.* 82 (1977) 2040–2044.
- [6] A. Bejan, *Convection Heat Transfer*, third ed., Wiley, Hoboken, 2004. pp. 586–591.
- [7] A. Bejan, K.R. Khair, Heat and mass transfer by natural convection in a porous medium, *Int. J. Heat Mass Transfer* 28 (1985) 909–919.
- [8] D.A. Nield, A. Bejan, *Convection in Porous Media*, third ed., V Springer, New York, 2006.
- [9] X.Q. Wang, A.S. Mujumdar, Heat transfer characteristics of nanofluids: a review, *Int. J. Thermal Sci.* 46 (2007) 1–19.
- [10] D.Y. Tzou, Instability of nanofluids in natural convection, *ASME J. Heat Transfer* 130 (2008) #072401.
- [11] D.Y. Tzou, Thermal instability of nanofluids in natural convection, *Int. J. Heat Mass Transfer* 51 (2008) 2967–2979.
- [12] D.A. Nield, A.V. Kuznetsov, The onset of convection in a nanofluid layer, *ASME J. Heat Transfer*, submitted for publication.
- [13] D.A. Nield, A.V. Kuznetsov, Thermal instability in a porous medium layer saturated by a nanofluid, *Int. J. Heat Mass Transfer* 52 (2009) 5796–5801.